Calculation for gamma ray buildup factor for aluminium, graphite and lead

Hiwa Mohammad Qadr

Department of Physics,
College of Science,
University of Raparin,
Sulaimanyah, Iraq
Email: hiwa.physics@uor.edu.krd

Abstract: The purpose of this work was to investigate and quantify the linear attenuation coefficient and the buildup factor for different materials. The linear attenuation coefficient of absorber materials such as graphite was (0.097 cm^{-1}), whereas it was observed (0.136 cm^{-1}) for aluminium, and lead was (0.596 cm^{-1}). By using the gamma radiation energies emitted from ^{60}Co source with 1332 keV, experimental and theoretical values are in a good agreement. Attenuation coefficient was measured by using counts of good geometry and bad geometry. The result shows that the linear attenuation is higher for lead and better radiation shielding compared with graphite and aluminium. Furthermore, buildup factor decreases with increasing thickness of the absorber material.

Keywords: sodium iodide detector; gamma attenuation; buildup factor; good geometry; graphite.

Reference to this paper should be made as follows: Qadr, H.M. (2019) 'Calculation for gamma ray buildup factor for aluminium, graphite and lead', *Int. J. Nuclear Energy Science and Technology*, Vol. 13, No. 1, pp.61–69.

Biographical notes: Hiwa Mohammad Qadr is Lecturer with a MSc degree in Physics and Technology of Nuclear Reactors, teaching in the College of Science at University of Raparin in Kurdistan Region, Iraq. His research interests focus on effects of radiation on materials, physics and materials of nuclear reactors and radiation protection.

1 Introduction

High-energy photons are one of the three main types of ionising radiation resulting from natural radioactivity (Buxton, 2008). They are an energetic form of electromagnetic radiation and occur in the form of gamma rays which interact with materials in a number of possible interactions, with three of these mechanisms playing a major role in the radiation detection processes (Krane and Halliday, 1988). These mechanisms of interaction are photoelectric effect, Compton scattering and pair production. The possibility of each mechanism depends on a number of factors, particularly the energy of the incident radiation. For instance, pair production can be the predominant interaction process if the energy of the incident gamma rays is higher than 1.02 MeV – twice the rest mass energy of an electron (Knoll, 2010).

Gamma ray attenuation coefficient is important in both applied and theoretical science (Hopkins et al., 2012). It is invaluable in many applied fields of science, such as nuclear medicine and diagnostics, radiation protection and dosimetry (Marashdeh et al., 2015), as well as industrial fields (Gökçe, 2019). Moreover, buildup factor is important for calculating absorbed dose, radiation shielding and protection, and has been investigated by many research groups (Akyildirim et al., 2017, Obaid et al., 2018, Sharaf and Saleh, 2015).

To begin with, attenuation coefficient is simply an expression for absorption probability of gamma rays in a certain material thickness (Rajasekhar and Kumar, 2014), while some gamma ray photons collide with electrons. As a result, absorption and scattering occur when some of the gamma rays pass through the material absorber. This scattering and absorption can be known as attenuation. The linear attenuation coefficient is defined as the fraction of an incident beam of gamma ray photons which is scattered or absorbed per unit thickness of the target absorber (Gjorgieva and Barandovski, 2016). In this work, the linear attenuation coefficient and gamma ray buildup factors were determined for graphite, aluminium and lead.

2 Theory

In this part of the work, I summarise theoretical relations which have been used for the determination linear attenuation coefficient, mass attenuation coefficient, Half Value Layer (HVL), Mean Free Path (MFP) and buildup factor. Basically, gamma rays are attenuated (interaction between the photon and the thickness of attenuation material) when the beam of gamma rays passes through an absorber. Some of the photons may travel through the thickness without interaction leading to the transmission of the photons. The transmitted beam at any thickness of the absorber is given by exponential equation (Kore, et al., 2016):

$$I = I_0 e^{-\mu x} \tag{1}$$

where μ is the linear attenuation coefficient of the absorber has unit of inverse centimetre (cm^{-1}). I_0 is the initial intensity of incident photons, I is the transmitted intensity of the radiation and x is the thickness. Rearrange of equation (1) for linear attenuation coefficient yields the following basic equation.

$$\mu = \frac{1}{x} \ln\left(\frac{I_0}{I}\right) \tag{2}$$

The linear attenuation coefficient is a sum of the attenuation coefficients for each type of interaction, as;

$$\mu = \mu_{ph} + \mu_C + \mu_P \tag{3}$$

where ph, C and P designate photoelectric effect, Compton scattering and pair production, respectively (Böke, 2014). The probability of interaction depends on the gamma ray photon energy, the density of medium and the nature of the material (Surung Bharat et al., 2016).

Mass attenuation coefficient can be a useful coefficient because only the atomic composition of the attenuator is taken into account and not the individual density of the material. Mass attenuation coefficient (μ_m) with unit $\left(\text{cm}^2/\text{g}\right)$ can be defined as a ratio of the linear attenuation coefficient to unit density (ρ) of the material (Saha, 2012). So, from linear attenuation coefficient, mass attenuation coefficient can be calculated by:

$$\mu_m = \frac{(\mu)}{(\rho)} \tag{4}$$

The HVL of a material can be defined as the thickness of the material at which the transmitted intensity is one-half the incident intensity for the gamma ray and depends on linear attenuation coefficient value (Agar et al., 2019). The HVL can be estimated using equation (5).

$$\text{HVL} = \frac{\ln 2}{\mu} \tag{5}$$

The MFP is the average distance between two successive collisions of gamma rays (Sayyed, et al., 2018), equation (6) has been used to calculate the MFP for the materials.

$$\text{MFP} = \frac{1}{\mu} \tag{6}$$

Buildup factor relies on linear attenuation, photon energy and shield thickness. Thus, it is important for gamma ray measurement (Akyildirim et al., 2017). Buildup factor can be defined as the ratio of the total radiation quantity at a given point to the number uncollided photons (Sharaf and Saleh, 2015).

Figure 1 shows narrow beam geometry (good geometry) with the absorber placed between the source and the detector. In this arrangement, the detector is able to detect only those photons that suffers no collision with the absorber. The equation (7) for good geometry can be written in the following expression.

$$\frac{I_{good}}{I_0} = e^{-\mu x} \tag{7}$$

Figure 1 Attenuation of gamma radiation under conditions of narrow beam geometry (good geometry)

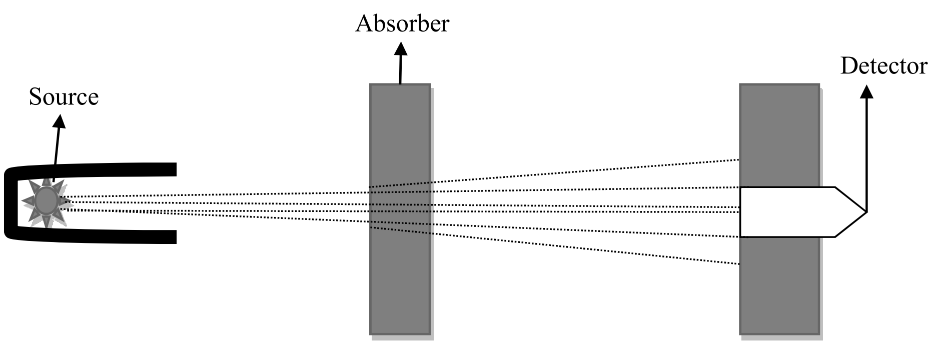

When scattered photons in the absorber are able to reach the detector, the geometrical arrangement called broad beam geometry (bad geometry) as shown in Figure 2. The equation (8) for bad geometry can be written in the following expression.

$$\frac{I_{bad}}{I_0} = e^{-\mu x} \tag{8}$$

Figure 2 Gamma ray photon attenuation under conditions of broad beam geometry (bad geometry)

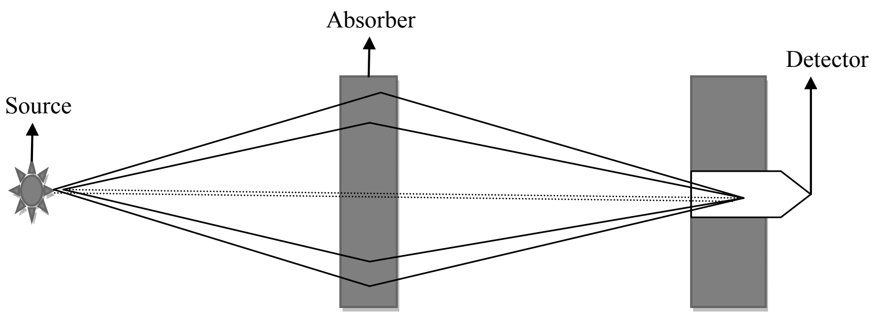

Hence, from equations (6) to (7), the buildup factor can be expressed in the following form (AL-Dhuhaibat, 2015).

$$B = \frac{I_{bad\ geometry}}{I_{good\ geometry}} \tag{9}$$

3 Experimental procedure

Figure 3 shows the block diagram for the electric system used in this paper. The materials used as the shield are aluminuim, lead and graphite. The radioactive source used is ^{60}Co which emits photon gamma radiation with energy 1332 keV. The energy spectra obtained from sodium iodide NaI (TI) detector were analysed by the maestro program.

Figure 3 Diagram of experimental set up

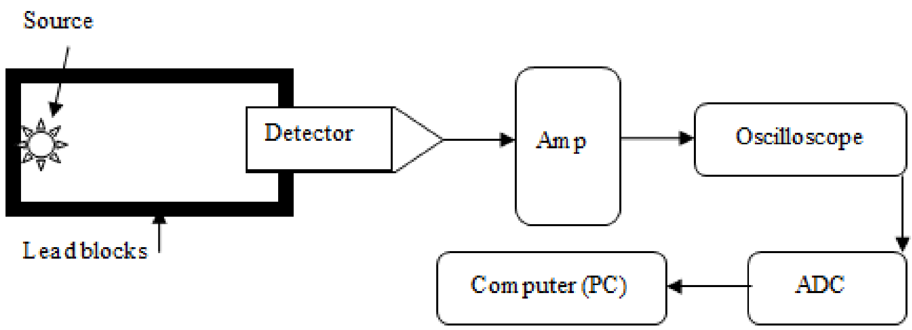

For good geometry, the materials was placed between the detector and the source. The maximum distance between the source and the absorber was 14 cm and the maximum distance between the detector and the source was 47 cm. The first reading was recorded without using any materials. Then, this step was repeated for different thicknesses. As a result of that, the detector was just able to detect the primary photons, which traverse the absorber without undergoing any collision.

For bad geometry, the distance between the source and the detector was increased to allow gamma photons to reach the detector after collisions. Thus, using different materials in both good and bad geometry, we can count numbers of gamma photons passing through these materials for various shield thickness.

4 Result and analysis

In this study, measurements of the attenuation coefficient for graphite, aluminium and lead at 1332 keV are carried out using narrow beam and broad beam geometries. Figures 4 to 6 show the Ln (I/I_0) as functions of the shielding thickness for three different materials.

Figure 4 The graph of Ln (I/I_0) against absorber thickness for graphite

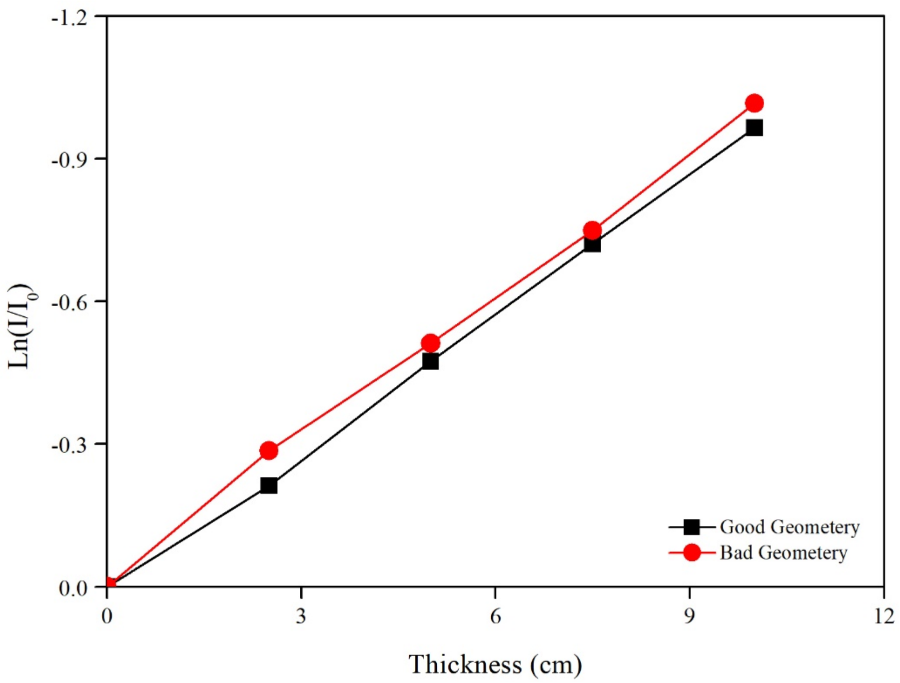

Figure 5 The graph of Ln (I/I_0) against absorber thickness for aluminium

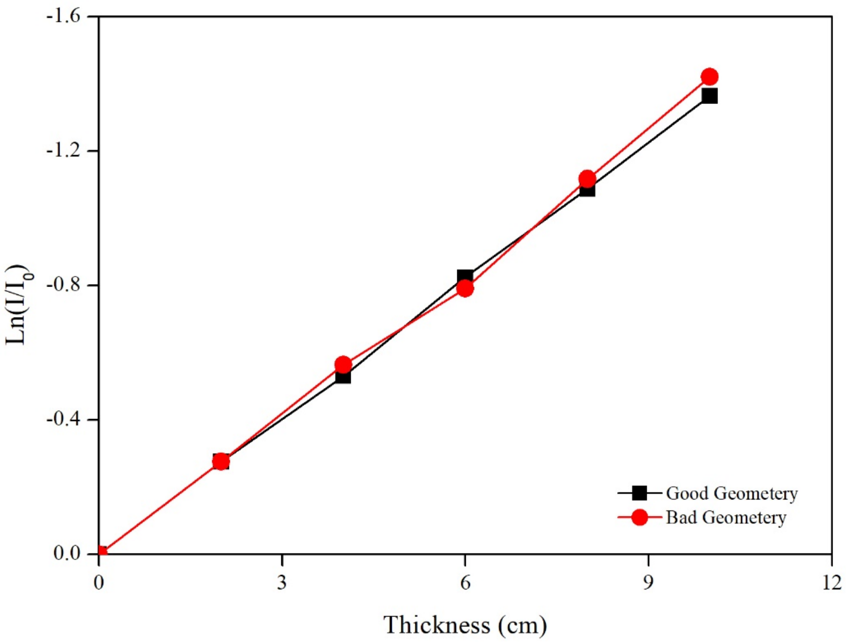

Figure 6 The graph of Ln (I/I_0) against thickness for lead

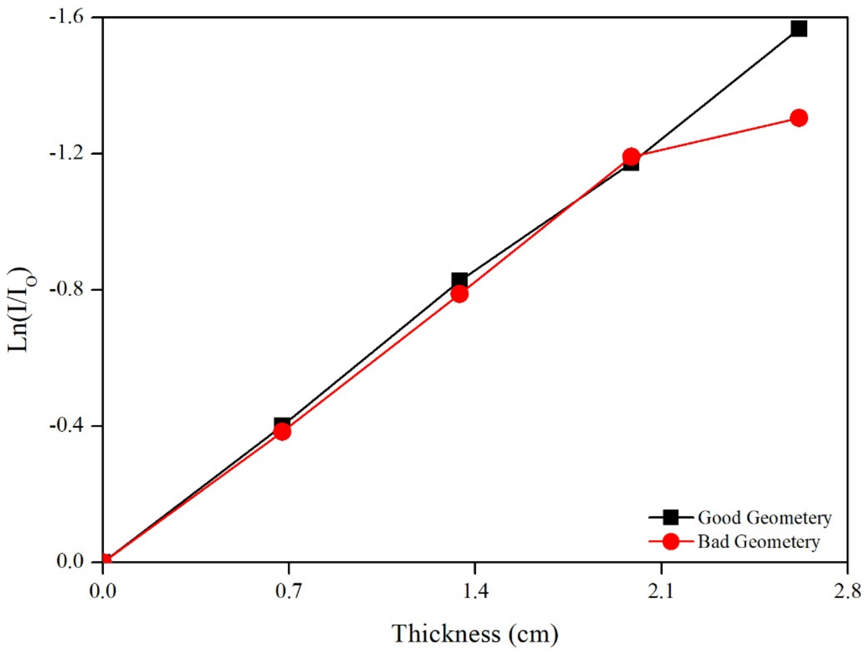

Table 1 shows the experimental results for the linear attenuation coefficient and mass attenuation coefficient for three types of shielding material. It is clear that the linear attenuation coefficient for lead has the highest value, and graphite the lowest. Higher values of the linear attenuation coefficient indicate lower penetration depth and higher probability of gamma ray interaction.

Table 1 Values of the experimental and calculated linear attenuation coefficient and mass attenuation coefficient for three types shielding material

Source	*Atomic Number*	ρ *(g/ cm^3)*	*Experimental* μ *(cm^{-1})*	*Calculated* μ *(cm^{-1})*	*Experimental* μ_m *(cm^2/g)*	*Calculated* μ_m *(cm^2/g)*
Graphite	6	2.25	0.097	0.116	0.043	0.052
Aluminium	13	2.74	0.136	0.137	0.0504	0.0501
Lead	82	11.34	0.596	0.592	0.0525	0.0522

The value of mass attenuation coefficient measured by equation (4). Lead also has higher value of the mass attenuation coefficient compared with aluminium and graphite. The calculated μ and μ_m values were compared the theoretical μ and μ_m values (Hubbell, 1969, Hubbell and Seltzer, 1995). It is clearly shown that there is a good agreement between the experimental and calculated data.

HVLs and MFP of the shielding materials are given in Table 2. It can be seen that the graphite has the highest value of the HVL and MFP. The values of theoretical and experimental HVL and MFP are a good agreement.

Table 2 Values of the experimental and calculated HVL and MFP for three types of shielding material

Source	*Experimental HVL (cm)*	*Calculated HVL (cm)*	*Experimental MFP (cm)*	*Calculated MFP (cm)*
Graphite	7.146	5.975	10.309	8.621
Aluminium	5.097	5.059	7.353	7.299
Lead	1.163	1.171	1.168	1.689

The buildup factors for single elements of graphite, aluminium and lead are measured using bad and good geometries at 1332 keV, and are shown in Table 3. The values of buildup factor for aluminium is lower than those for graphite and lead. The value of buildup factor depends on the atomic number and the thickness of the shielding material. Therefore, increasing atomic number can cause a decrease in the value of buildup factor. However, atomic number of the lead is higher than aluminium. But, the values of shielding thickness for lead are lower than aluminium that was used in this experiment.

Table 3 Values of good and bad geometry and buildup factors for graphite, aluminium and lead

Graphite			
Thickness (cm)	*Bad geometry*	*Good geometry*	*Buildup factor*
0	304.6633	131.3233	2.319949
2.5	228.8467	106.1867	2.155135
5	182.5667	81.76667	2.232777
7.5	144.1033	63.87	2.256197
10	110.2367	50.02333	2.203706

Table 3 Values of good and bad geometry and buildup factors for graphite, aluminium and lead (continued)

Aluminium			
Thickness (cm)	*Bad geometry*	*Good geometry*	*Buildup factor*
0	292.6033	148.7733	1.966773
2	222.1233	112.89	1.967608
4	166.3867	87.53	1.900911
6	132.6733	65.22667	2.034035
8	95.76	50.12667	1.91036
10	70.71	38.03	1.859322
Lead			
Thickness (cm)	*Bad geometry*	*Good geometry*	*Buildup factor*
0	297.95	132.1833	2.254067
0.675	203.1767	88.41667	2.297946
1.341	135.4767	57.78667	2.344428
1.986	90.60667	40.89333	2.215683
2.617	80.89	27.59333	2.931506

5 Conclusions

In this work, the attenuation properties of three types of shielding material have been evaluated and discussed in terms of attenuation coefficient and buildup factor at 1332 keV. The values of the linear attenuation coefficient decrease with increasing atomic number and density of material. Therefore, lead appears as a good shielding material due to its higher value for linear attenuation coefficient. The data showed good agreement between experimental and theoretical results.

Obviously, the values of bad geometry are greater than the values of good geometry, because when the geometry is bad there are more scattered photons. On the other hand, there are no scattered photons for good geometry. It is observed that the buildup factor for graphite has higher value because it has a lower atomic number compared to other materials .Accordingly, more work needs to be done to verify if extremely gamma ray sources instead of one radioactive source when ^{60}Co used.

References

Agar, O., Sayyed, M., Tekin, H., Kaky, K.M., Baki, S. and Kityk, I. (2019) 'An investigation on shielding properties of BaO, MoO3 and P2O5 based glasses using MCNPX code', *Results in Physics*, Vol. 12, pp.629–634.

Akyildirim, H., Waheed, F., Günoğlu, K. and Akkurt, İ. (2017) 'Investigation of Buildup Factor in Gamma-Ray Measurement', *Acta Physica Polonica A*, Vol. 132, pp.1203–1206.

AL-Dhuhaibat, M.J.R. (2015) 'Study of the shielding properties for some composite materials manufactured from polymer epoxy supported by cement, aluminum, iron and lead against gamma rays of the cobalt radioactive source (Co-60)', *International Journal of Application or Innovation in Engineering and Management*, Vol. 4, No. 6, pp.90–98.

Böke, A. (2014) 'Linear attenuation coefficients of tissues from 1 keV to 150 keV', *Radiation Physics and Chemistry*, Vol. 102, pp.49–59.

Buxton, G.V. (2008) 'An overview of the radiation chemistry of liquids', *Radiation Chemistry from Basics to Applications in Material and Life Sciences*.

Gjorgieva, S. and Barandovski, L. (2016) Measurement of the mass attenuation coefficient from 81 keV to 1333 keV for elemental materials Al, Cu and Pb', *AIP Conference Proceedings*, AIP Publishing, doi: 10.1063/1.4944211.

Gökçe, H.S. (2019) 'High temperature resistance of boron active belite cement mortars containing fly ash', *Journal of Cleaner Production*, Vol. 211, pp.992–1000.

Hopkins, D.N., Maqbool, M. and Islam, M.S. (2012) 'Linear attenuation coefficient and buildup factor of MCP-96 alloy for dose accuracy, beam collimation, and radiation protection', *Radiological Physics and Technology*, Vol.5, pp.229–236.

Hubbell, J. (1969) *Photon Cross Sections, Attenuation Coefficients and Energy Absorption Coefficients*, National Bureau of Standards Report NSRDS-NBS29, Washington, DC.

Hubbell, J.H. and Seltzer, S.M. (1995) *Tables of X-ray mass attenuation coefficients and mass energy-absorption coefficients 1 keV to 20 MeV for elements Z= 1 to 92 and 48 additional substances of dosimetric interest*, National Institute of Standards and Technology-PL, Gaithersburg, MD. Available online at: http://physics.nist.gov/PhysRefData/XrayMassCoef/cover.html

Knoll, G.F. (2010) *Radiation Detection and Measurement*, John Wiley & Sons

Kore, P.S., Pawar, P.P. and Selvam, T.P. (2016) 'Evaluation of radiological data of some saturated fatty acids using gamma ray spectrometry', *Radiation Physics and Chemistry*, Vol. 119, pp.74–79.

Krane, K.S. and Halliday, D. (1988) *Introductory Nuclear Physics*, Section 9.6, Wiley, New York.

Marashdeh, M.W., Al-Hamarneh, I.F., Munem, E.M.A., Tajuddin, A., Ariffin, A. and Al-Omari, S. (2015) 'Determining the mass attenuation coefficient, effective atomic number, and electron density of raw wood and binderless particleboards of Rhizophora spp. by using Monte Carlo simulation', *Results in Physics*, Vol. 5, pp.228–234.

Obaid, S.S., Sayyed, M., Gaikwad, D. and Pawar, P.P. (2018) 'Attenuation coefficients and exposure buildup factor of some rocks for gamma ray shielding applications', *Radiation Physics and Chemistry*, Vol. 148, pp.86–94.

Rajasekhar, E. and Kumar, R.J. (2014) 'Experimental investigation of gamma radiation shielding characteristics of wood', *International Journal of Humanities*, Vol. 2, pp.21–26.

Saha, G.B. (2012) *Physics and Radiobiology of Nuclear Medicine*, Springer Science & Business Media

Sayyed, M., Tekin, H., Kılıcoglu, O., Agar, O. and Zaid, M. (2018) 'Shielding features of concrete types containing sepiolite mineral: comprehensive study on experimental, XCOM and MCNPX results', *Results in Physics*, Vol. 11, pp.40–45.

Sharaf, J. and Saleh, H. (2015) 'Gamma-ray energy buildup factor calculations and shielding effects of some Jordanian building structures', *Radiation Physics and Chemistry*, Vol. 10, pp.87–95.

Surung Bharat, S., Lokhande Rajkumar, M. and Pawar Pravina, P. (2016) 'Linear attenuation coefficient and mean free path in the energy range of 0.1 MeV to 1.5 MeV', *International Journal of Applied Research*, Vol. 2, pp.279–283.